PROCEEDINGS OF SCIENCE

Heavy Flavor Spectroscopy Studies at ATLAS

Vincenzo Canale on behalf of ATLAS Collaboration[a,*]

[a] *Università di Napoli - FEDERICO II and INFN,*
Department of Physics,
Via Cintia, 80124 Naples, Italy

E-mail: vincenzo.canale@unina.it, vincenzo.canale@cern.ch

Results from ATLAS studies on heavy flavor spectroscopy are presented. The results of the analyses on four-muons final states in pp collisions are presented at the different LHC energies $\sqrt{s} = 8\,\text{TeV}$ and $\sqrt{s} = 13\,\text{TeV}$, and in particular in the channels $(\Upsilon(\rightarrow \mu^+\mu^-) + \mu^+\mu^-)$ and di-charmonium (di-J/Ψ and $J/\Psi + \Psi_{2S}$) decaying to muon pairs.

12th Large Hadron Collider Physics Conference (LHCP2024)
3-7 June 2024
Boston, USA

*Speaker

PoS(LHCP2024)074

1. Introduction

1.1 The physics context

Since the discovery of X(3872) in 2003 [1] the exciting era of the un-conventional hadronic physics started with an increasing evidence of new tetra-quarks (TQ) and penta-quark (PQ) states [2], which triggered a very large number of theoretical investigations on the behaviour of the strong interactions. For dynamical reasons, the heavy quark masses strongly suppress $Q\bar{Q}$ production from vacuum, then the presence of heavy flavour (HF) doublets ($Q\bar{Q}$) in the final states is an excellent hint for searching and interpreting these exotic states like tetra-quarks T($Q\bar{Q}Q\bar{Q}$) ([3]-[5]). In addition, several extensions of the Standard Model foresee the presence of new particles decaying to four leptons via mechanisms involving quarkonium final states ([6]-[9]). Moreover, the experimental signature of heavy quarkonia, via well identifiable physics states (e.g. $J/\psi \to \mu^+\mu^-$ and $\Upsilon \to \mu^+\mu^-$), is certainly more effective in the complex LHC hadronic environment. Therefore, ATLAS studied the four muon final states in pp collisions at LHC, via quarkonia final states and for different invariant mass ($m_{4\mu}$) ranges.

1.2 The data samples, the detector performances and trigger

ATLAS is a multipurpose apparatus to study pp interactions at LHC, the detailed description of the detector can be found in Ref. [10]. The analyzed data sample corresponds to the integrated luminosities of 21.3 fb^{-1} at $\sqrt{s}$ = 8 TeV in 2012 and 140 fb^{-1} at $\sqrt{s}$ = 13 TeV in (2015-2018).

Regarding the analysis on HF, the main detector components are: (a) the Muon System (MS) with tracking capability up to pseudorapidity $|\eta| \leq 2.7$, with momentum resolution $\sigma_{p_T}/p_T = 0.1$ up to 1 TeV; (b) the Inner Detector (ID) which reconstructs tracks up to $|\eta| \leq 2.5$ with efficiency $\epsilon_{trk} = 0.99$ and momentum resolution $\sigma_{p_T}/p_T = 0.0004 p_T(\text{GeV}) + 0.0015$. The vertexing accuracy (primary and secondary) results in a resolution on the track impact parameter of about 10 μm. The invariant mass distributions are the key-tool for these analyses; the typical resolutions are in the range 50 MeV to 100 MeV for $\mu\mu$ pairs, and the observed signal/background ratios are high.

The trigger for HF physics is based on muons up to $|\eta| \leq 2.4$, with several combinations of transverse momentum thresholds ($p_T^{(\mu)} \geq 4,\ 6$ GeV) and multiplicity. Depending on the increasing background conditions, also charge and invariant mass requirements and prescaling are applied [11].

2. Search for narrow low-mass resonances in the four-muon final state

To optimize both the physics interest (e.g. tetraquarks or scalar/pseudoscalar Higgs-like particles) and the experimental signature, the search is performed in the four-muon final state via the decay chain $X \to \Upsilon + \mu^+\mu^- \to \mu^+\mu^-\mu^+\mu^-$ in the range $m_{4\mu} \in [10, 50]$ GeV. The trigger requires more than 2 or 3 muons with $p_T \geq 4$ GeV, but with different configurations for the various data taking period: (a) at $\sqrt{s}$ = 8 TeV a combination of un-prescaled 2-μ and 3-μ corresponfing to $\mathcal{L}$=20.3 fb^{-1}, (b) at $\sqrt{s}$ = 13 TeV pre-scaled 3-μ corresponding to $\mathcal{L}$=51.5 fb^{-1}, (c) at $\sqrt{s}$ = 13 TeV only 3-μ with pair of opposite charge and $m_{\mu^+\mu^-} \in [8, 12]$ GeV for $\mathcal{L}$ =58.5 fb^{-1}. The reconstruction proceeds with the identification of a vertex with four *identified*[1] muons with two opposite sign

[1]The identification criteria of muons are described in [12].

charge pairs (OS), one of them compatible with a decay $\Upsilon \rightarrow \mu^+\mu^-$; the different steps with the detailed selection criteria are reported in [13]. Figure 1 shows the $m_{4\mu}$ distributions, in the range [10, 50] GeV, obtained for the data samples at different energies:

- the data at $\sqrt{s} = 8$ TeV (Figure 1a) exhibit two excesses, at $m_{4\mu} \sim 18$ GeV and $m_{4\mu} \sim 21$ GeV, over the background which can be estimated from events with the Υ candidates and a same sign charge muon pair (SS). Several simulation studies, removing the muon identification criteria, did not show evidence for artificial peaks [13]. Moreover, the $m_{4\mu}$ distributions for OS but with Υ candidates selected in the side-bands (Figure 1b), did not present any excess;
- the excesses are not present at $\sqrt{s} = 13$ TeV as shown in Figures 1c and 1d; the OS and SS shapes are equivalent, an enhancement in OS selection was noticed in part of the sample due to the opposite sign trigger requirements. The data show that the combinatorial background is significantly larger (factor ~ 2.5) per unit of integrated luminosity at $\sqrt{s} = 13$ TeV with respect to $\sqrt{s} = 8$ TeV.

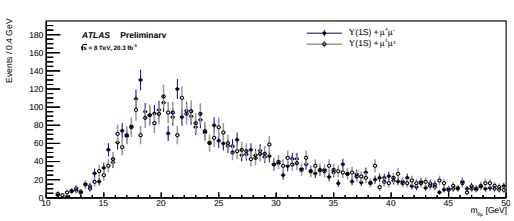

(a) $\sqrt{s} = 8$ TeV (2012): OS and SS combinations

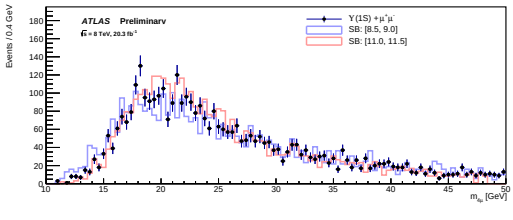

(b) $\sqrt{s} = 8$ TeV (2012): OS and Υ side-bands combinations

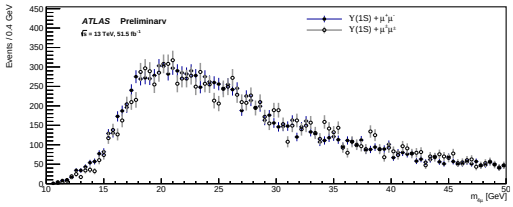

(c) $\sqrt{s} = 13$ TeV (2015-17): OS and SS combinations

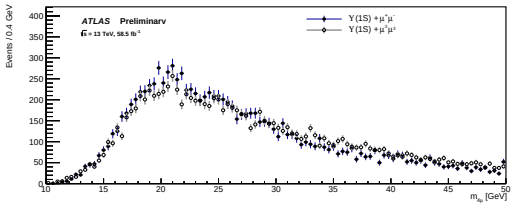

(d) $\sqrt{s} = 13$ TeV (2018): OS and SS combinations

Figure 1: $m_{4\mu}$ distributions from [13]

An unbinned maximum-likelihood fit procedure is used to assess the compatibility of the $m_{4\mu}$ distribution with the background-only hypothesis. The signal is described by a gaussian centered at m_X with $\sigma_X = 0.2$ GeV (detector resolution), the background is parametrized with fourth-order Chebyshev polynomials. The fits are performed in sliding $m_{4\mu}$ windows of $\Delta m_{4\mu} = 10$ GeV around the test mass m_X between 15-45 GeV with a step size of 0.05 GeV. The local p-value, when testing a hypothesised resonance at m_X, is based on the profile likelihood ratio test statistic; it is calculated using the asymptotic approximation [14]; local and global significance values are calculated accounting for the trial factors or the look-elsewhere effect of the search range [15].

As shown in Figure 2a, for the $\sqrt{s} = 8$ TeV data, the smallest p-value is at $m_X = 18.05$ GeV with significance 5.5σ (4.6σ global). The effects of the variation of the fit range $\Delta m_{4\mu}$ in the interval [6,12] GeV and of the parametrization of signal and background shapes [13] correspond

to the shaded band in the Figure. The result for the fit in the $m_{4\mu}$ range [15-25] GeV is shown in Figure 2b. An extensive study of cut variations in the different steps of the analysis, with respect to the baseline, was carried out to test the stability of the apparent excess [13]; in terms of significance the excursion was between $(3.6 \div 6.3)\sigma$ ($(1.9 \div 5.4)\sigma$ global).

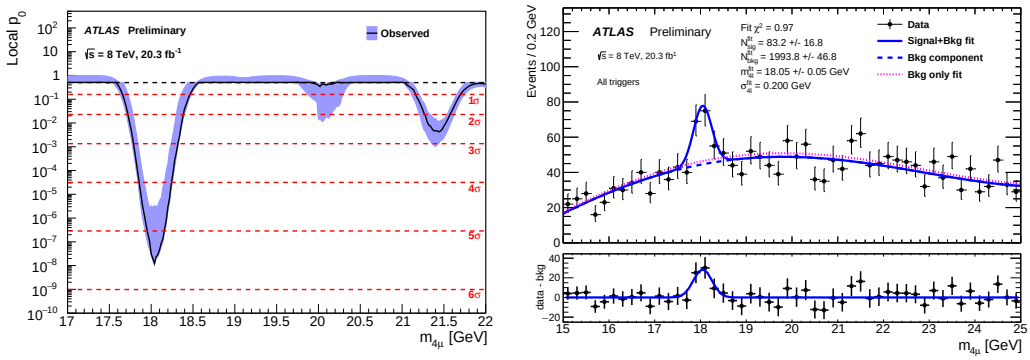

(a) compatibility with backgound only hypothesis **(b)** fit resul for the $m_{4\mu}$ range [15-25] GeV

Figure 2: Statistical results for analysis of $\sqrt{s} = 8$ TeV data from [13]

The data at $\sqrt{s} = 13$ TeV provide an independent and blinded sample to check the observed excess at $m_X = 18.05$ GeV at $\sqrt{s} = 8$ TeV; the same selection is used and the $m_{4\mu}$ distribution is fitted in the range [15-25] GeV, but no significant excess is observed in the samples. The observed upper limits at 95% CL and the median expected (68% and 95%) CL intervals, for $\sigma \cdot \mathrm{BR}(X \to \Upsilon(\to \mu^+\mu^-) + \mu^+\mu^-)$, are obtained with the CLs construction [16] with a signal model of fixed $m_X = 18$ GeV and width of 0.2 GeV. The results are shown in Figure 3, there is a large model-uncertainty for any interpretation due to the dependence on reconstruction efficiency of the signal (e.g. few benchmark models with low/high reconstruction efficiencies are reported). The limits at different energies are not directly comparable; the picture is consistent with results from LHCB [17] and CMS[18], though those collaborations did not observe any excess.

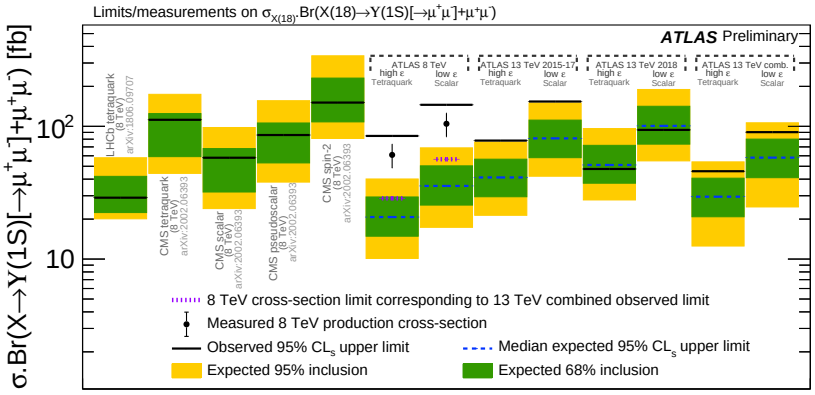

Figure 3: Comparison of the different limits for $\sigma \cdot \mathrm{BR}(X \to \Upsilon(\to \mu^+\mu^-) + \mu^+\mu^-)$ from [13]

3. Di-charmonium events in the four-muon final state

To search for new heavy tetra quarks states ($T_{Q\bar{Q}Q\bar{Q}}$), ATLAS studied the di-charmonium events decaying to four muons ($J/\Psi \to \mu^+\mu^- + J/\Psi \to \mu^+\mu^-$) and ($J/\Psi \to \mu^+\mu^- + \Psi_{2s} \to \mu^+\mu^-$). The data sample corresponds to an integrated luminosity of 140 fb^{-1} at $\sqrt{s}$ = 13 TeV. The trigger requires either two OS muons with invariant mass compatible with J/y or Ψ_{2S} (mass range [2.5,4.3] GeV) or three muons containing at least one such di-muon pair. The efficiency, for a TQ with $m_X \simeq 7$ GeV, is 72%. The reconstruction proceeds with the identification of a vertex with four *identified* muons with two opposite sign charge pairs, compatible with the decays $J/\Psi \to \mu^+\mu^-$ ($m_{\mu\mu} \in [2.94, 3.25]$ GeV) or $\Psi_{2S} \to \mu^+\mu^-(m_{\mu\mu} \in [3.56, 3.80]$ GeV); the detailed steps of the selection are reported in [19]. To enhance the signal/background ratio, an angular requirement of $\Delta R = \sqrt{\Delta\eta^2 + \Delta\varphi^2} \leq 0.25$ is applied. The background analysis (validation and normalization) is performed in dedicated control regions (CR: $\Delta R > 0.25$) and then transfer factors are used to obtain the yields in the signal region (SR: $\Delta R \leq 0.25$). The main sources of background are: (a) non-prompt charmonium production from B-hadron decays ($B\bar{B} \to J/\Psi + J/\Psi(\Psi_{2S}) + x$): (b) prompt single charmonium and non-resonant 2-μ production; (c) double charmonium production from single(double) parton scattering (S[D]PS) [20]. The feed-down component from $\Psi_{2S} \to$ "X'' $\to J/\Psi + x$ is also taken into account. Figure 4 shows the $m_{4\mu}$ distributions for the SRs; a significant excess near the threshold is observed, similarly to CMS [21] and LHCb [22] whose $X(6900)$ signal contribution is inserted in the plot.

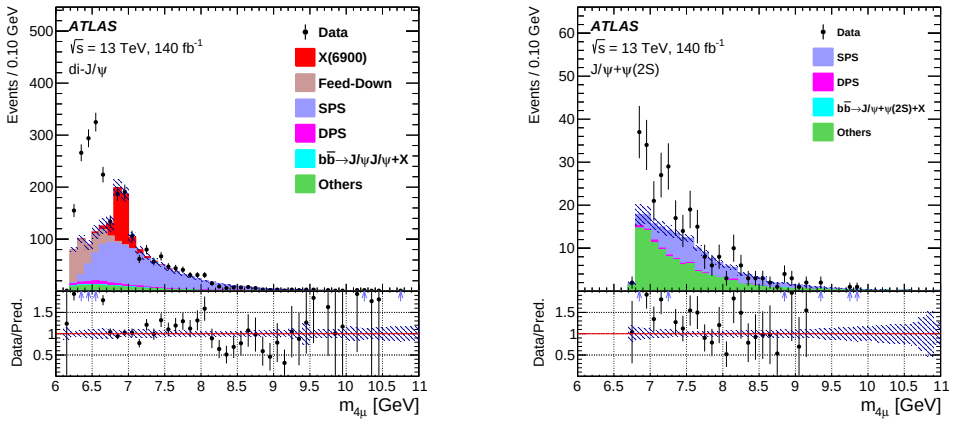

(a) $(J/\psi + J/\Psi)$ sample **(b)** $(J/\psi + \Psi_{2S})$ sample

Figure 4: $m_{4\mu}$ distributions for di-charmonium candidates in SR ($\Delta R \leq 0.25$) from [19]

The $m_{4\mu}$ data distibutions, for both the SR and CR simultaneously, were fitted with an unbinned maximum likelihood, taking into account the signal and background contibutions and the nuisance parameters which account for systematic uncertainties shared between the two regions and are constrained from subsidiary mesurements. Two models were used to parametrize the signal:

- in the di-J/Ψ sample, the model A contains three interfering Breit-Wigner resonances; while the model B contains only two independent ones, but one interferes with the SPS background;

- in the $(J/\Psi + \Psi_{2S})$ sample, the model α contains the previous fixed three resonances of di-J/Ψ and a fourth independent one; while the model β assumes a single resonance.

In all cases, the phase-space factor and the detector resolution are taken into account. The $m_{4\mu}$ mass spectra fit to the data, in the two channels, are shown in Figure 5. The fitted masses and widths of the resonances are given in Figure 6a. Both the significance of all resonances, and the one for $X(6900)$ alone, far exceed the 5σ significance level computed with the asymptotic formula based on the profile likelihood ratio [14]. The systematic uncertainties in the fitted masses and widths of the highest resonances in models A and α of the two channels are summarized in Figure 6b.

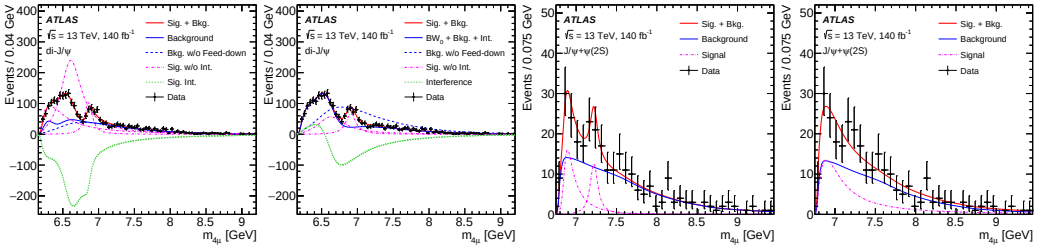

(a) **(b)** **(c)** **(d)**

Figure 5: The fit results from [19] for di-J/Ψ ([a] model A, [b] model B) and $(J/\psi + \Psi_{2S})$ ([c] model α, [d] model β).

di-J/ψ	model A	model B
m_0	$6.41 \pm 0.08^{+0.08}_{-0.03}$	$6.65 \pm 0.02^{+0.03}_{-0.02}$
Γ_0	$0.59 \pm 0.35^{+0.12}_{-0.20}$	$0.44 \pm 0.05^{+0.06}_{-0.05}$
m_1	$6.63 \pm 0.05^{+0.08}_{-0.01}$	—
Γ_1	$0.35 \pm 0.11^{+0.11}_{-0.04}$	
m_2	$6.86 \pm 0.03^{+0.01}_{-0.02}$	$6.91 \pm 0.01 \pm 0.01$
Γ_2	$0.11 \pm 0.05^{+0.02}_{-0.01}$	$0.15 \pm 0.03 \pm 0.01$
$\Delta s/s$	$\pm 5.1\%^{+8.1\%}_{-8.9\%}$	—
J/ψ+ψ(2S)	model α	model β
m_3	$7.22 \pm 0.03^{+0.01}_{-0.04}$	$6.96 \pm 0.05 \pm 0.03$
Γ_3	$0.09 \pm 0.06^{+0.06}_{-0.05}$	$0.51 \pm 0.17^{+0.11}_{-0.10}$
$\Delta s/s$	$\pm 21\%^{+25\%}_{-15\%}$	$\pm 20\% \pm 12\%$

(a)

Systematic Uncertainties (MeV)	di-J/ψ m_2	di-J/ψ Γ_2	J/ψ+ψ(2S) m_3	J/ψ+ψ(2S) Γ_3
Muon calibration	±6	±7	<1	±1
SPS model parameter	±7	±7	<1	
SPS di-charmonium p_T	±7	±8	<1	
Background MC sample size	±7	±8	±1	<1
Mass resolution	±4	−3	−1	$^{+2}_{-4}$
Fit bias	−13	+10	$^{+9}_{-10}$	$^{+50}_{-16}$
Shape inconsistency	<1		±4	±6
Transfer factor	—		±5	±23
Presence of 4th resonance	<1		—	
Feed-down	$^{+4}_{-1}$	$^{+6}_{-2}$	—	
Interference of 4th resonance	—		−32	−11
P and D-wave BW	+9	+19	<1	±1
ΔR and muon p_T requirements	$^{+3}_{-2}$	$^{+6}_{-4}$	$^{+1}_{-2}$	−2
Lower resonance shape	—		$^{+3}_{-7}$	$^{+31}_{-34}$

(b)

Figure 6: From [19]: (a) the fitted masses and natural width (in GeV); (b) the different sources of systematic uncertainites

In both channels, the details of the lower-mass structure cannot be discerned directly from the data, and other interpretations (e.g., multiple non-interfering resonances, reflection effects and threshold enhancements) cannot be excluded. More data are required to better characterize the excesses observed in both channels.

4. Conclusion

ATLAS studied four-muon final states in pp collisions at LHC. An excess was observed at 8 TeV around $m_{4\mu} \approx 18$ GeV in the final state $\Upsilon(\rightarrow \mu^+\mu^-) + \mu^+\mu^-$); but at 13 TeV the data do not support this signal. At 13 TeV, in the final states di-J/Ψ and $(J/\Psi + \Psi_{2S})$, ATLAS confirmed the evidence of X(6900) seen by CMS and LHCb, and observed a significant excess above the kinematic production threshold which is compatible with the presence of new states decaying to di-J/Ψ.

References

[1] Belle Collaboration, Phys. Rev. Lett. 91 (2003) 262001.

[2] S. L. Olsen, T. Skwarnicki, and D. Zieminska, Rev. Mod. Phys. 90 (2018) 015003.

[3] A. V. Berezhnoy, A. K. Likhoded and A. A. Novoselov, Phys. Rev. D87 (2013) 054023.

[4] W. Chen, H.-X. Chen, X. Liu, T. Steele and S.-L. Zhu, Phys. Lett. B 773 (2017) 247.

[5] M. Karliner, S. Nussinov and J. L. Rosner, Phys. Rev. D 95 (2017) 034011.

[6] S. Gopalakrishna, S. Jung and J. D. Wells, Phys. Rev. D 78 (2008) 055002.

[7] V. Kartvelishvili, A. V. Luchinsky and A. A. Novoselov, Phys. Rev. D 79 (2009) 114015.

[8] U. Ellwanger, C. Hugonie and A. M. Teixeira, Phys. Rept. 496 (2010) 1.

[9] D. Curtin, R. Essig, S. Gori and J. Shelton, JHEP 02 (2015) 157.

[10] ATLAS Collaboration, JINST 3 (2008) S08003.

[11] ATLAS Collaboration, JINST 15 (2020) P09015.

[12] ATLAS Collaboration, Eur. Phys. J. C 81 (2021) 578.

[13] ATLAS Collaboration, ATLAS-CONF-2023-041, url: https://cds.cern.ch/record/2869238

[14] G. Cowan et al., Eur. Phys. J. C 71 (2011) 1554.

[15] E. Gross and O. Vitells, Eur. Phys. J. C70 (2010) 525.

[16] A. L. Reed, J. Phys. G 28 (2002) 2693.

[17] LHCb Collaboration, JHEP 10 (2018) 086.

[18] CMS Collaboration, Phys. Lett. B 808 (2020) 135578.

[19] ATLAS Collaboration, Phys. Rev. Lett. 131 (2023) 151902.

[20] T. Sjöstrand et al., Comput. Phys. Commun. 191 (2015) 159.

[21] CMS Collaboration, Phys. Rev. Lett. 132 (2024) 111901.

[22] LHCb Collaboration, Sci. Bull. 65 (2020) 1983.